Electronic Structure of Friedel–Crafts Catalysts, an *ab initio* Study of the RF–BF_3 Adducts

Arturo Arnau,[a] **Juan Bertrán,**[b] **and Estanislao Silla**[a,*]
[a] *Departamento de Química Física, Universidad de Valencia, Doctor Moliner 50, 46100 Burjassot (Valencia), Spain*
[b] *Departamento de Química, Universitat Autònoma de Barcelona, 08193 Bellaterra (Barcelona), Spain*

By means of *ab initio* calculations using several basis sets (STO-3G, 3-21G, and 6-31+G), the minimum-energy structures for the RF–BF_3 intermediates (R = H, Me, and Et) of the Friedel–Crafts alkylation reaction have been obtained. The role of the catalyst in the process through an analysis of dissociation energies, atomic charges, and LUMO energies of reaction intermediates, and the same quantities for the RF species, has been studied.

RF–BF_3 adducts have been widely utilized in studies on Friedel–Crafts alkylation.[1] RF–BF_3 adducts have been isolated by Olah *et al.* and have been used in studies on the mechanism of aromatic electrophilic substitution.[2,3] Theoretical studies on these systems[4–6] avoid the problem that the presence of d-orbitals causes the majority of Lewis acids, and are some of the few papers that try to give a theoretical interpretation of homogeneous catalysis.

An *ab initio* study[4] using the STO-3G and 4-31G basis set on the HF–BF_3 system led to the following conclusions. (a) The energy needed to break heterolytically the HF bond in the isolated HF molecule is much larger than that needed to break it in the HF–BF_3 adduct. (b) The changes in electronic distribution owing to the formation of a dative bond between the Lewis acid and the base favour a larger positive charge on the hydrogen atom, thus allowing for an improvement in the electrophilicity of HF. However, the most interesting Friedel–Crafts reactions are alkylations, where differences appear when the alkyl group changes.

A first attempt to analyse the specificity of the different alkyl groups was carried out by means of the MINDO/3 method. The RF–BF_3 species were studied (R = H, Me, Et, Pr, and Pr^i).[6] Use of this semiempirical method allowed us to explore much of the potential energy hypersurface. A series of cyclic structures that suggested a mechanism for halogenoalkane isomerization in the presence of Lewis acids was obtained. However, as we have pointed out,[6] the MINDO/3 method is subject to severe limitations.[7,8] Exploration of the CH_4 + HF system has allowed us to check that these cyclic structures are likely to be a consequence in the MINDO/3 method. Thus, we think that a reinvestigation of the series with an *ab initio* method is needed.

In this work we have examined, fairly completely, the potential-energy hypersurface for the species RF–BF_3 (R = H, Me, and Et) with an STO-3G basis set, which provides a good computing rate and is quite efficient for analytic gradient geometry optimizations.[9] Minima found with this basis set have been further optimized with the 3-21G split-valence basis set, which improves the results in spite of a somewhat longer computing time. Finally, for the R = H and R = Me cases, we have recalculated these structures with a 6-31 + G basis set. All results have been analysed to interpret the role played by BF_3 as a catalyst, since its presence in the adducts leads to an increase in the alkyl group charge, a diminution of the LUMO energy, a variation in the R–F bond distance, and a lowering of the heterolytic cleavage energy.

Method of Calculation.—Exploration of the potential-energy hypersurface with the STO-3G minimal basis set[10] has been carried out with a gradient full-geometry optimization, by means of the FORCE program.[11]

Optimizations with the 3-21G split-valence basis set[12] of the structures found previously have been performed with the MONSTERGAUSS program[13] by means of the optimally conditioned optimization method of Davidson.[14] In both cases, optimizations were stopped when the root-mean-square gradient was smaller than 5×10^{-4} mdyn.† Calculations with the 6-31+G basis set[15] were carried out with the GAUSSIAN 86 program.[16] Computations were performed with a VAX 8300 computer.

Results and Discussion

RF–BF_3 *Adduct Structure.*—Analysis of the RF–BF_3 species potential energy hypersurface led to the detection of two minima. The most stable is depicted in Figure 1A. This structure is very close to that found in a restricted optimization in previous work[4] where the other minimum was not found. The other minimum is very similar to that represented in Figure 1A, though the HFBH dihedral angle becomes 180°, which leads to a difference energy between both minima of 2.1 kJ mol^{-1}. Between these two located minima there is a transition state with a BFH angle of 179.4°, a B–FH bond length of 2.02 Å, and an energy 31.3 kJ mol^{-1} higher than that of the absolute minimum. The main component of its transition vector is associated with the BFH angle.

For the MeF–BF_3 species, similar minimum-energy structures are also found. In Figure 1B we show the structure corresponding to the absolute minimum. A second minimum, close in energy to the first one, also appears in this case (with a difference of 0.8 kJ mol^{-1}), where the only noticeable change with respect to the most stable one (Figure 1B) is that the FBFC dihedral angle changes from 180 to 0°. A transition state with a BFC angle of 180° and a B–FMe bond length of 2.06 Å also appears, the energy of which is 21.5 kJ mol^{-1} higher than that of the absolute minimum.

For the EtF–BF_3 species, the higher complexity of the molecule with respect to previous species leads to more minima being found in the potential-energy hypersurface. In Figure 1C the structure corresponding to the absolute minimum is depicted.

In Figure 2 we show the structures obtained starting from the STO-3G minima of the three species studied, when carrying out a geometry optimization using the 3-21G basis set. From a geometrical point of view, the most noticeable fact with respect

---

† 1 dyn = 10^{-5} N.

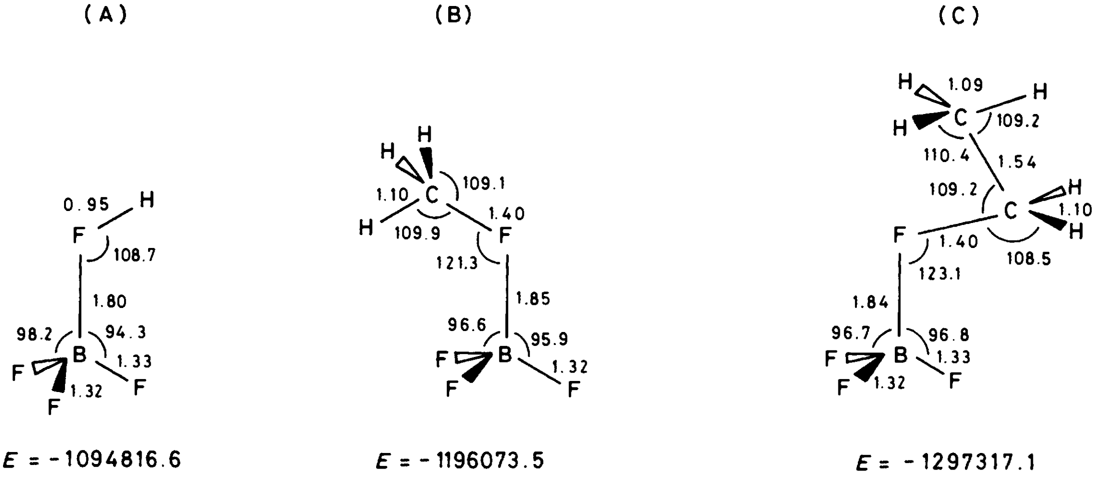

Figure 1. Energies (in kJ mol^{-1}) and structures for the absolute minima detected in the STO-3G potential energy hypersurface of the RF–BF$_3$ species (R = H, Me, and Et) (distances in Å, bond angles in °).

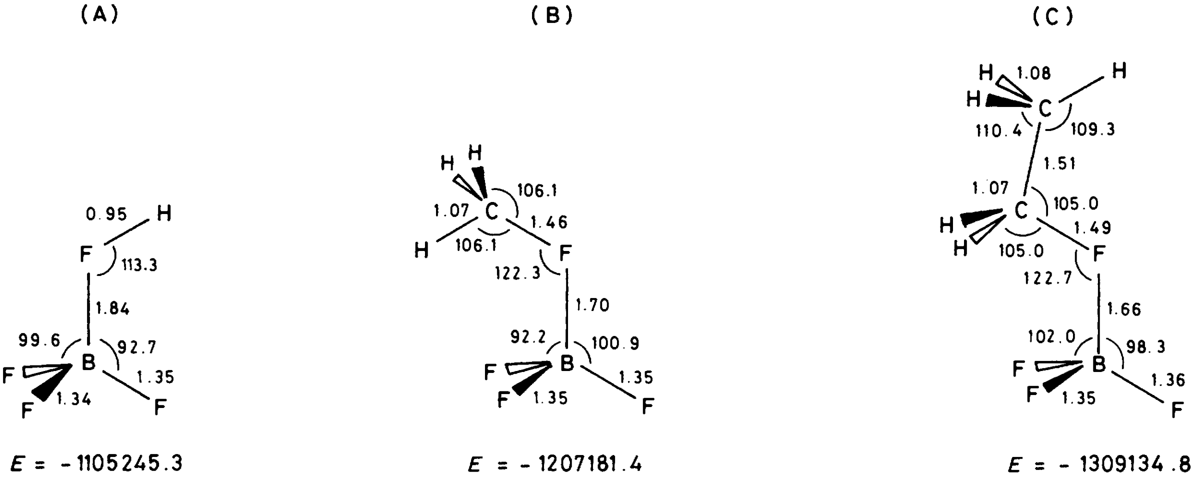

Figure 2. Energies (in kJ mol^{-1}) and structures for the 3-21G basis set found with the geometry optimization of the RF–BF$_3$ minima calculated with the minimal basis set (Figure 1).

Table 1. Stabilization energies (in kJ mol^{-1}) (E) and bond overlap populations of the RF–B (P) and R–F (P') bonds, for the RF–BF$_3$ species (R = H, Me, and Et), computed with the STO-3G and 3-21G basis sets.

	E		P		P'	
Species	STO-3G	3-21G	STO-3G	3-21G	STO-3G	3-21G
HF–BF$_3$	61.6	77.4	0.064	0.078	0.204	0.210
MeF–BF$_3$	41.7	84.8	0.056	0.090	0.214	0.146
EtF–BF$_3$	45.4	95.5	0.059	0.096	0.212	0.131

Table 2. Net charges on group R (in e units) for the RF–BF$_3$ species (R = H, Me, and Et) obtained with the STO-3G and 3-21G basis sets.

Species	STO-3G	3-21G
HF–BF$_3$	0.29	0.52
MeF–BF$_3$	0.25	0.54
EtF–BF$_3$	0.28	0.55

to the results depicted in Figure 1 is the change in the CFBF dihedral angle in the EtF–BF$_3$ species, and the lengthening of the C–F bond and the shortening of the B–FR one, either for R = Me or R = Et, whereas in the HF–BF$_3$ species a lengthening in the B–FH bond is produced.

All changes point towards formation of stronger adducts with a higher stabilization energy when using 3-21G basis set, as indicated in Table 1. This difference in stability is lower for the HF–BF$_3$ adduct, which can be related to geometrical changes observed in Figures 1 and 2, and to variations in the RF–B bond overlap populations, which are also shown in Table 1.

Adducts of the RF–BF$_3$ type have been detected and isolated experimentally[2] for several alkyl fluorides; their electric conductivities have been measured, and are higher for larger groups R. One can thus deduce that the ionic character increases when advancing along the homologous series RF–BF$_3$. These experimental results agree with the structures obtained with both basis sets, especially that with the 3-21G set. Since the RF–BF$_3$ species ionize by RF bond cleavage, lengthening of this bond and shortening of the RF–B bond when going from R = Me to R = Et coincides with the increase in ionic character of these species, as demonstrated also by the bond overlap population values of RF–B and R–F (Table 1), and the net charge on group R (Table 2).

Role of the Catalyst.—Once the structures obtained for the intermediates RF–BF$_3$ from the Friedel–Crafts alkylation

Table 3. Dissociation energies (in kJ mol^{-1}) for the RF and RF–BF$_3$ species (R = H, Me, and Et), and their differences, computed with the STO-3G, 3-21G, and 6-31+G basis sets.

Process	STO-3G	3-21G	6-31+G
$HF \longrightarrow H^+ + F^-$ (1)	2 511.5	1 806.6	1 517.3
$MeF \longrightarrow Me^+ + F^-$ (2)	2 027.9	1 314.4	969.2
$EtF \longrightarrow Et^+ + F^-$ (3)	1 921.2	1 224.8	
$HF\text{–}BF_3 \longrightarrow H^+ + BF_4^-$ (1′)	1 681.2	1 215.8	1 137.8
$MeF\text{–}BF_3 \longrightarrow Me^+ + BF_4^-$ (2′)	1 188.6	731.0	613.6
$EtF\text{–}BF_3 \longrightarrow Et^+ + BF_4^-$ (3′)	1 076.7	652.1	
$\Delta_{1-1'}$	830.3	590.8	379.5
$\Delta_{2-2'}$	839.3	583.4	355.6
$\Delta_{3-3'}$	844.5	572.7	

Table 4. Differences in the charge of group R (in *e* units) between the RF–BF$_3$ and RF species (R = H, Me, and Et), obtained with the STO-3G, 3-21G, and 6-31+G basis sets.

R	STO-3G	3-21G	6-31+G
H	0.12	0.07	0.07
Me	0.10	0.13	0.06
Et	0.12	0.14	

Table 5. LUMO energy (in kJ mol^{-1}) for the RF and RF–BF$_3$ species (R = H, Me, and Et), obtained with the STO-3G, and 6-31+G basis sets.

	E_{LUMO}		
Species	STO-3G	3-21G	6-31+G
HF	1 435.5	688.7	483.1
MeF	1 565.6	731.5	206.7
EtF	1 506.4	718.7	
HF–BF$_3$	1 136.7	487.0	107.4
MeF–BF$_3$	1 103.6	547.4	126.4
EtF–BF$_3$	1 105.4	552.4	

reaction have been described, we will focus our attention on the interpretation of the catalytic role of BF$_3$ in the process.

In the first place, we shall perform an energy analysis of the RF and RF–BF$_3$ species bond cleavage, to investigate the easier dissociation of the latter and hence its stronger power as an alkylating agent. If one compares the two processes (A) and (B):

$$RF \longrightarrow R^+ + F^- \qquad (A)$$

$$RF\text{–}BF_3 \longrightarrow R^+ + BF_4^- \qquad (B)$$

the energy needed for the heterolytic cleavage of the RF bond is much lower for reaction (B) than for (A), for all cases and all basis sets (Table 3). The presence of anionic species, in particular F$^-$, requires an improvement in the basis sets used previously. For that reason, for R = H and R = Me we have carried out several calculations using the 6-31 + G basis set. This basis set gives a value of 392.1 kJ mol^{-1} for the BF$_3$ affinity for the F$^-$ ion, whereas the STO-3G calculations give 891.2 kJ mol^{-1} and the 3-21G calculations give 669.5 kJ mol^{-1}. The experimental value has been estimated[17] to be 297.1 kJ mol^{-1}. Inclusion of R = Et would lead to a tremendous increase in central processing unit time, while the conclusions are not likely to be very different from the other cases.

These results show that in Friedel–Crafts alkylations with alkyl fluorides, abstraction of the alkyl group requires a smaller energy in the presence of the catalyst. The big difference between the values of the three columns of Table 3 reflects the different quality of the basis sets employed. We think nevertheless that the big increase in dissociation energy obtained with all basis sets is enough to show the effectiveness of BF$_3$ as a catalyst.

Another fact which can give us an idea about the role of the catalyst in this process is the comparison between the charge supported by the alkyl group in the RF species and the charge supported when the RF–BF$_3$ intermediate complex between the RF species and the catalyst has already been formed. Results are shown in Table 4. One can see that, for all basis sets and all species studied, a clear increase in the alkyl-group charge appears when the catalyst is bonded to RF. These changes in atomic population will correspond to the greater electrophilic character of the adduct with respect to RF, at least in the initial phases of the attack on a given substrate.

Finally, we studied the role of the catalyst by analysing the lowest unoccupied molecular orbital (LUMO) of the found species. While alkylation is being performed, the alkylating agent is transferred to the aromatic substrate, and separation of the R group from the remainder of the attacking complex RF–BF$_3$ then occurs. Furthermore, this electrophilic attack is accompanied by a charge transfer from the nucleophile towards the electrophile. Both aspects, breakage of R and charge transfer, can be interpreted by the frontier orbital theory. With regard to the electrophile, it is the LUMO that will play a leading role in the process.

We have checked in all structures of the RF–BF$_3$ species presented in Figures 1 and 2, and, with all basis sets employed in this work (STO-3G, 3-21G, and 6-31+G), the overlap of the atomic orbitals involved in the R–BF$_4$ bond with a larger participation in the LUMO is clearly antibonding. Thus, when the LUMO is being occupied along the alkylation process, a weakening of the studied bond will be found. This will finish in the scission of the alkylating agent from the BF$_4$ group.

Another factor, also kinetic, may help one to study the power of the intermediates as alkylating agents, *viz.* their LUMO energy. The lower it is, the easier the electron transfer will be carried out. In Table 5 we give the LUMO energies for the RF and RF–BF$_3$ species. It must be pointed out that all LUMO energies are positive. One can see that a noticeable stabilization of the RF–BF$_3$ LUMOs is found with respect to LUMOs of the corresponding RF. Thus, the former species are more likely to accept the electrons appearing in the alkylation process.

Finally, from a dynamic point of view, the two aspects mentioned in the frontier orbital study are linked. Since the LUMO is antibonding between the R and BF$_4$ groups, cleavage means a progressive stabilization of the LUMO, which leads to a larger charge transfer, which in turn contributes to the cleavage of the alkylating agent in the Friedel–Crafts reaction.

Acknowledgements

This work was supported by the CAICYT, Project no. 714/84. E. S. thanks Prof. I. Nebot for helpful comments.

References

1 'Friedel–Crafts and Related Reactions,' ed. G. A. Olah, Interscience, New York, 1964.
2 G. A. Olah, S. J. Khun, and J. A. Olah, *J. Chem. Soc.*, 1957, 2174.
3 G. A. Olah and S. J. Khun, *J. Am. Chem. Soc.*, 1958, **80**, 6535.
4 E. Silla, E. Scrocco, and J. Tomasi, *Theor. Chim. Acta*, 1975, **40**, 343.
5 G. Alagona, E. Scrocco, E. Silla, and J. Tomasi, *Theor. Chim. Acta*, 1977, **45**, 127.
6 F. Mora, J. Bertrán, and E. Silla, *J. Chem. Soc., Perkin Trans. 2*, 1982, 647.
7 R. C. Bingham, M. J. S. Dewar, and D. H. Lo, *J. Am. Chem. Soc.*, 1975, **97**, 1307.
8 M. J. S. Dewar and H. S. Rzepa, *J. Am. Chem. Soc.*, 1978, **100**, 58.

9 E. R. Davidson and D. Feller, *Chem. Rev.*, 1986, **86**, 681.
10 W. J. Hehre, R. F. Stewart, and J. A. Pople, *J. Chem. Phys.*, 1969, **51**, 2657.
11 H. Bernhard, *QCPE*, Program no. 427, University of Indiana.
12 J. S. Binkley, J. A. Pople, and W. J. Hehre, *J. Am. Chem. Soc.*, 1980, **102**, 939.
13 M. Peterson and R. Poirier, Program MONSTERGAUSS, University of Toronto, Ontario, Canada, 1983.
14 N. C. Davidson, *Math. Prog.*, 1975, **9**, 1, modified by Mike and Kathy Peterson, University of Toronto, Ontario, Canada.
15 R. H. Nobes, W. R. Rodwell, and L. Radom, *J. Comput. Chem.*, 1982, **3**, 561.
16 M. J. Frisch, J. S. Binkley, H. B. Schlegel, K. Raghavachari, C. F. Melius, R. L. Martin, J. J. P. Stewart, F. W. Bobrowicz, C. M. Rohlfing, L. R. Kahn, D. J. Defrees, R. Seeger, R. A. Whiteside, D. J. Fox, E. M. Flender, and J. A. Pople, 'GAUSSIAN 86', Carnegie-Mellon University, Pittsburgh PA, 1984.
17 J. C. Haartz and D. H. McDaniel, *J. Am. Chem. Soc.*, 1973, **95**, 8562.

Received 12*th May* 1988; *Paper* 8/01868E